Bioactivity of ceramic–polymer composites with varied composition and surface topography

S. M. REA*, S. M. BEST, W. BONFIELD
Department of Materials Science and Metallurgy, University of Cambridge, Pembroke Street, Cambridge CB2 3QZ, UK
E-mail: smr31@cam.ac.uk

HAPEX™ (40 vol % hydroxyapatite in a high-density polyethylene matrix) and AWPEX (40 vol % glass–ceramic apatite–wollastonite in a high-density polyethylene matrix) are composites designed to provide bioactivity and to match the mechanical properties of human cortical bone. HAPEX™ has had clinical success in middle ear and orbital implants, and there is great potential for further orthopaedic applications of these materials. However, more detailed *in vitro* investigations must be performed to better understand the biological interactions of the composites. In this study, the bioactivity of each material was assessed. Specifically, the effects of controlled surface topography and ceramic filler composition on apatite layer formation in acellular simulated body fluid (SBF) with ion concentration similar to those of human blood plasma were examined. Samples were prepared as $1 \times 10 \times 10\,mm^3$ tiles with polished, roughened or parallel-grooved surface finishes, and were incubated in 20 ml of SBF at 36.5 °C for one, three, seven or 14 days. The formation of an apatite layer on the composite surface after immersion was demonstrated by thin-film X-ray diffraction, environmental scanning electron microscopy and energy dispersive X-ray analysis. Variations in sample weight and solution pH over the period of incubation were also recorded. Significant differences were found between the two materials tested, with greater bioactivity in AWPEX than HAPEX™. Results also showed surface topography to be important, with rougher samples correlated to earlier apatite formation. Osteoblast-like cells proliferated favourably on both composite materials, with many filopodia connections, preferential attachment to ceramic particles and contact guidance effects evident.

1. Introduction

Recent advances in bone replacement have often focussed on ceramic–polymer composites. One such material, HAPEX™, consists of 40 vol % hydroxyapatite (HA) in a high-density polyethylene (PE) matrix [1]. In another, known as AWPEX, the filler phase is glass–ceramic apatite–wollastonite (A–W) [2]. These composites have been designed to provide bioactivity and to match the mechanical properties of human cortical bone. Clinical success has been seen with HAPEX™ in middle ear and orbital implants [3, 4], and there is great orthopedic potential for these materials. However, more detailed *in vitro* information is desirable to better understand the biological interactions of the composites, assessing not only the effects of the different ceramic components for the two materials, but also the effects of surface topography.

One important area of material analysis, assessed in this study, is overall bioactivity. A common characteristic of all bioactive implants, thought to play a key role in direct bone bonding, is the formation of a surface hydroxy–carbonate apatite layer when implanted. The formation of an apatite layer *in vitro* is also found on the surfaces of various bioactive glasses and ceramics after immersion in acellular simulated body fluid (SBF) [5, 6]. SBF contains ion concentrations close to those in blood plasma and the formation of an apatite layer on the surface of a material in SBF can be used to predict *in vivo* bioactivity. In this work, the *in vitro* surface structure change and hence bioactivity of HAPEX™ and AWPEX composites with different topographies after immersion in SBF were studied. As a basis of comparison, untreated HAPEX™ and AWPEX were also examined through scanning electron microscopy (SEM), environmental SEM (ESEM), X-ray diffraction and surface profilometry measurements.

As a complement to SBF study, preliminary osteoblast-like cell culture experiments were also performed to qualitatively examine the attachment and morphology of cells on the material surfaces. Active osteoblasts are bone-forming cells, laying down new unmineralised bone matrix and playing a role in mineralisation through the secretion of calcium-rich structures known as matrix vesicles [7]. By studying these cells in an isolated and

*Author to whom all correspondence should be addressed.

controlled *in vitro* environment, an initial understanding of the interactions of the materials and cells can be reached while avoiding possible complications of *in vivo* research [8]. Although *in vitro* experiments may differ from the *in vivo* situation [9], they have been well correlated with implant studies [10] and are an important starting point for investigation.

2. Materials and methods

2.1. Materials

The polymer phase used for all composites was high-density PE in the form of Rigidex blow moulding grade HM4560 XP, from BP Chemicals Ltd., Middlesex, UK (molecular weight of 225 000; density of 945 kg/m^3). P88 grade HA, with a mean particle size of 3.9 μm and d_{10}–d_{90} spread of 0.4–7.7 μm, was obtained from Plasma Biotal Ltd., Tideswell, UK, and produced via a continuous precipitation process using calcium hydroxide as the precursor. Glass–ceramic A–W, with a mean particle size of 4.5 μm and d_{10}–d_{90} spread of 0.3-15 μm, was supplied by Nippon Electric Glass Co. Ltd., Osaka, Japan, produced by crystallisation of a glass powder.

For both HAPEX™ and AWPEX composites, ceramic filler at 40 vol % was incorporated into high-density PE using a Betol co-rotating twin-screw extruder model BTS40L. Each composite was extruded through a 1 cm round die into air and quickly cooled in a deionised water bath at 20 °C, then cut to 1 cm lengths, frozen in liquid nitrogen, and ground in a Glen Creston ultra centrifuge mill. The powdered composites were finally formed into plates using a flash-type mould and Palamine hydraulic hot plate press. Samples measuring $1 \times 10 \times 10\,mm^3$ were created from these plates using an Accutom® precision saw at a cutting speed of 0.5 mm/s. Surfaces of these samples were either left as-cut or polished through successive abrasion levels down to 1-μm diamond grit.

To create grooved surfaces, polished samples were mounted with wax onto a fixed holder with the polished face parallel to a precision diamond wire saw (Well Diamond Wire Saws, Inc., Le Locle, Switzerland) with a wire diameter of 170 μm and lateral control to 5 μm. Parallel grooves were inscribed into the material by pressing the sample into the rotating wire, with separations between grooves of 0.3 or 1.0 mm.

2.2. Analysis of untreated composites

For surface imaging of materials prior to SBF incubation, each sample was mounted onto an SEM stub with double-sided carbon tape and sputter coated with gold. Imaging was performed on a JSM-820 microscope, with accelerating voltages varied from 5 to 15 kV for secondary and back-scattered electron analyses. Uncoated samples were also secured onto holders and imaged in a JEOL XL30 ESEM at an accelerating voltage of 5 kV, with elemental composition and distribution assessed using an energy dispersive X-ray (EDX) attachment.

The surface roughness values for all topographic finishes of HAPEX™ and AWPEX samples were determined by surface profilometry using a WYCO NT-2000 system (Wyco Corporation, Tucson, USA). A minimum of eight separate samples of each material were tested, to give a final averaged result.

2.3. Bioactivity in SBF

Samples of HAPEX™ and AWPEX with polished or roughened surfaces were immersed in separate plastic ware containers with 20 ml of SBF solution [11] each and incubated at 37 °C. For HAPEX™, samples were also tested with parallel 100-μm grooves. After soaking for one, three, seven or 14 days, the substrates were removed from the fluid, washed with distilled water and air-dried.

The pH of aliquots of the SBF after incubation with the different samples was measured at each time point using an electrolyte-type pH meter (CamLab Ltd., Cambridge, UK). The weight change of the composites with time was also determined as an indicator of the reaction stage of the interaction of the composites with SBF. Weights of each specimen before (w_i) and after (w_f) SBF soak as measured by analytical balance were recorded, with soaked samples removed from solution and allowed to air dry before being weighed. The percentage weight change of the samples $(\Delta w\%)$ was calculated as:

$$\Delta w\% = 100 \times \frac{w_f - w_i}{w_i} \quad (1)$$

Thin-film X-ray diffraction (TF-XRD) measurements were performed on Siemens D500 equipment using Cu Kα ($\lambda = 0.15405$ nm) radiation as the source, at a rate of $2\theta = 2°$/min with 0.1 slits and a glancing angle of 1° against the incident beam on the composite surface. Data were collected from 15 to 40°, with operation parameters of 40 kV and 40 mA.

Uncoated HAPEX™ and AWPEX samples removed from solution and allowed to air dry at one, three, seven and 14 day time points throughout SBF incubation were secured onto holders and imaged in a JEOL XL30 ESEM at an accelerating voltage of 5 kV. Elemental composition and distribution through X-ray mapping were performed with an EDX attachment.

2.4. Cell culture and SEM imaging

MG-63 osteoblast-like cells (European Collection of Cell Cultures, Salisbury, UK; ECACC No. 86051601) at passage numbers below four were cultured in Dulbecco's Modified Eagle Medium, supplemented with 10% heat-inactivated foetal bovine serum (FBS) and 1% glutamine (glu). Cells were seeded onto HAPEX™ and AWPEX samples at densities ranging from 0.3 to 2.5×10^4 cells/cm^2, as determined by hemocytometer count using Trypan blue dye (Flow Laboratories, Inc., McLean, USA) to exclude non-viable cells. Incubation periods between seeding and examination varied from one to five days. A range of seeding densities and of incubation times was selected to allow imaging of cell attachment and morphology at different levels of confluence and development, with both materials tested under the same sets of conditions.

Samples were sterilised by gamma irradiation at 2.5 Mrad (Isotron Plc., Swindon, UK), prior to use in

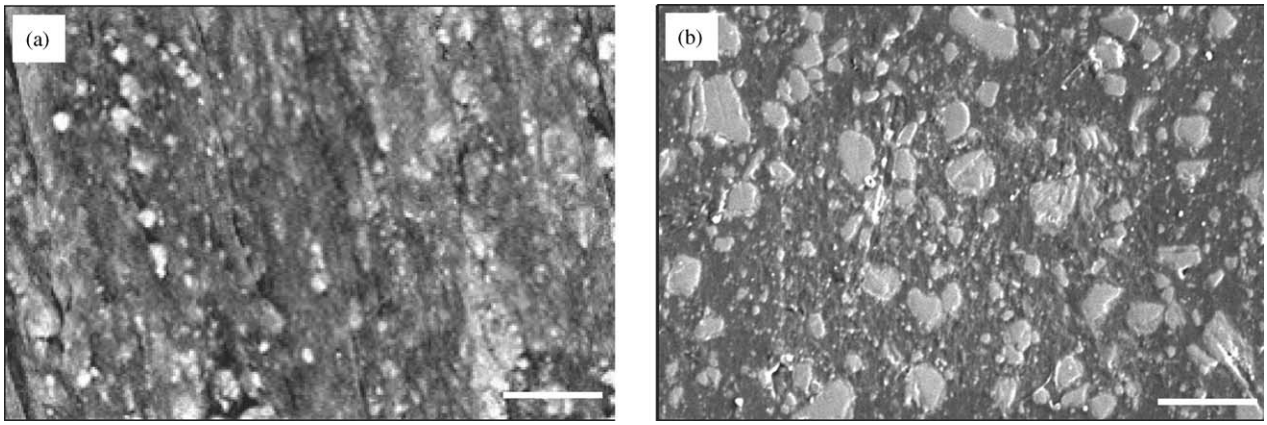

Figure 1 SEM backscattered electron images of (a) as-cut HAPEX™ and (b) polished AWPEX. Both scale bars 10 μm.

cell culture, and were further pre-treated by a 48 h soak in 70% ethanol to remove endotoxins. Endotoxins are lipopolysaccharide (LPS) components of the outer cell wall of gram-negative bacteria such as *E. coli*, *Salmonella* and other leading pathogens, and may be picked up easily from the surrounding environment. LPS elicits a variety of inflammatory responses *in vivo* and can affect cell culture studies at levels as low as 19 pg/ml [12]. Common sterilisation methods of irradiation do not affect endotoxin particles. However, extended treatment with alcohol as employed in this study has been shown to be effective [13].

For SEM imaging, cells were transported under bicarbonate-buffered medium, then rinsed twice by dipping quickly in ice-cold water and immediately frozen in liquid nitrogen. These samples were freeze-dried overnight, mounted onto SEM stubs with double-sided carbon tape, and sputter coated with carbon. Imaging was performed on a FEI-Philips XL30 FEG SEM with accelerating voltages varied from 2 to 15 kV for secondary and backscattered electron analyses.

3. Results

3.1. Analysis of untreated composites

HAPEX™ samples, both left as-cut and subsequently polished, maintained a homogenous distribution of HA particles within the PE matrix of the composite as shown by backscattered electron imaging at 15 kV (Fig. 1(a)). However, as expected, significant differences in surface morphology could be seen in secondary electron images taken at 5 kV, with as-cut samples exhibiting greater roughness. SEM examination of AWPEX gave similar morphological information (Fig. 1(b)), showing homogeneous particle distribution in all samples, with differences in roughness between as-cut and polished surfaces.

For HAPEX™ samples grooved using a diamond wire saw, although some variations in groove and ridge width were seen across the length of the samples, general production was found to be good. Grooves were approximately 150 μm in width with clear profiles and with lateral separation by polished ridge regions as desired (Fig. 2).

X-ray mapping analyses of HAPEX™ and AWPEX samples prior to SBF incubation are shown in Figs. 3 and 4, respectively. For all surface finishes, carbon (C) content was high. Oxygen (O), calcium (Ca) and phosphorus (P) were also found in all samples, especially within the ceramic components, with silicon (Si) and magnesium (Mg) also present at detectable levels in AWPEX composites.

Overall surface roughness parameters of samples with different surface finishes are listed in Table I. From these results, it can be seen that polished samples had much less surface roughness than as-cut samples, as in previous study [14]. Furthermore, as-cut samples had lower surface roughness than grooved samples. Surface roughness parameters were not significantly different between HAPEX™ and AWPEX samples of the same surface finish.

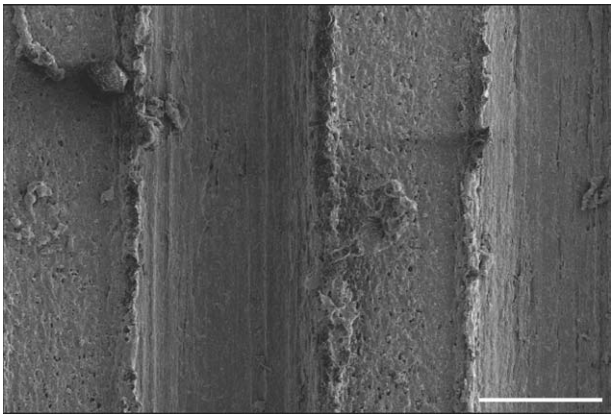

Figure 2 SEM secondary electron image of grooves created using a diamond wire saw in HAPEX™. Scale bar 100 μm.

TABLE I Surface profilometry parameters for HAPEX™ and AWPEX composites with as-cut, polished and grooved surface finishes

Material		R_a (nm)	R_q (nm)
HAPEX™	As-cut	622 ± 180	792 ± 210
	Polished	106 ± 13	137 ± 18
	Grooved	1616 ± 1300	2577 ± 2000
AWPEX	As-cut	627 ± 210	822 ± 260
	Polished	104 ± 12	141 ± 19

Data shown as mean ± standard deviation for $N = 8$. R_a = arithmetic average roughness height, R_q = root mean square average roughness height, both over entire surface.

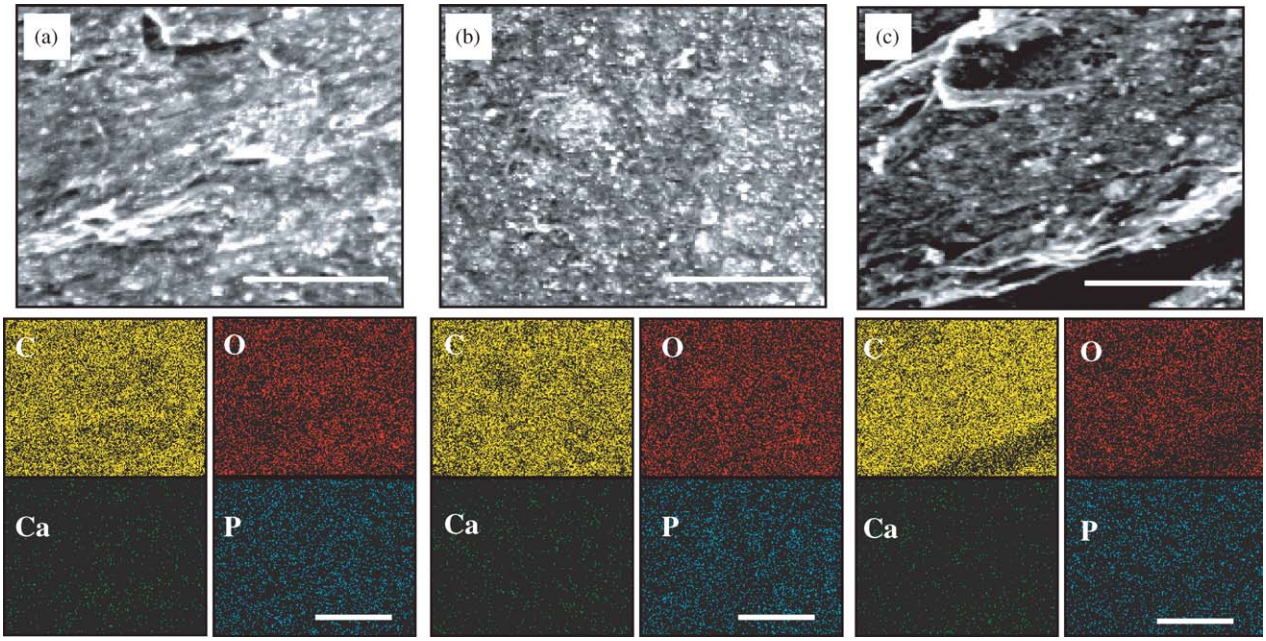

Figure 3 SEM imaging and X-ray mapping of (a) as-cut, (b) polished and (c) grooved HAPEX™. All scale bars 10 μm.

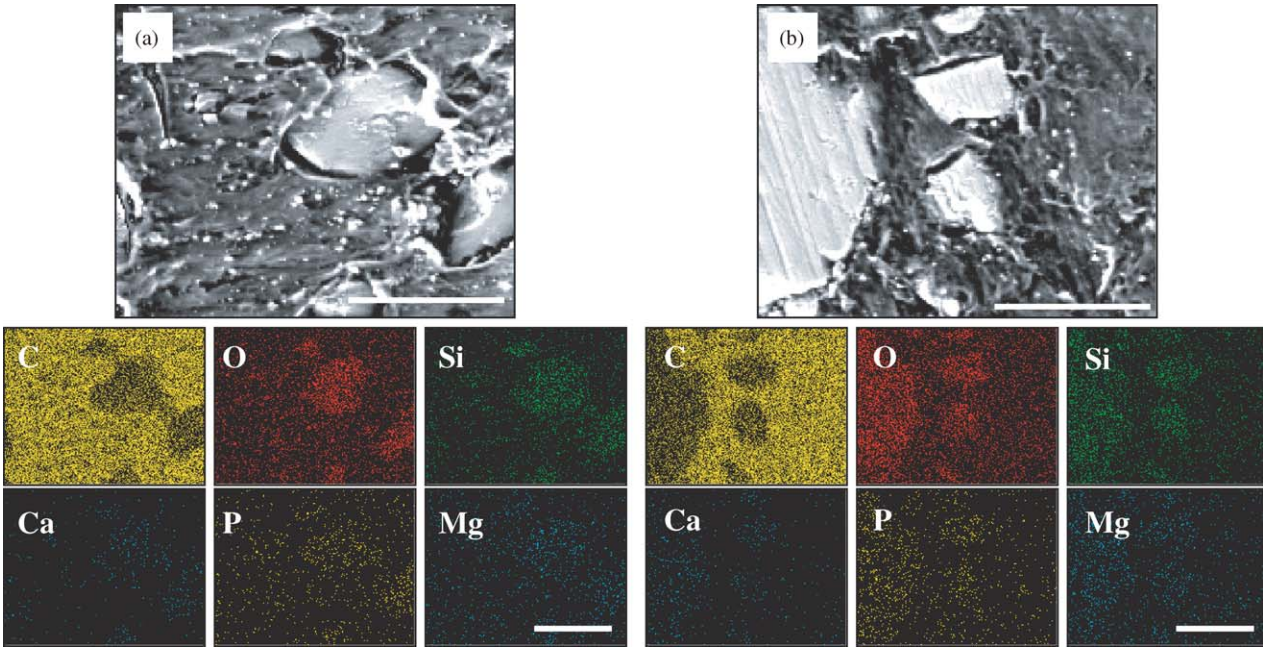

Figure 4 SEM imaging and X-ray mapping of (a) as-cut and (b) polished AWPEX. All scale bars 10 μm.

3.2. Bioactivity in SBF

Little change was seen in the SBF incubated with HAPEX™ and AWPEX samples for all times up to 14 days, with solution pH staying within $\pm$ 0.15 of the initial 7.40 level for all cases. All samples increased in weight over the period of SBF incubation. This increase was most noticeable in as-cut samples, although results in all cases indicated only small changes of less than 1.5% of the initial sample weight. Polished AWPEX samples indicated a slight decrease in sample weight at one day, but this decrease was not seen for HAPEX™ samples of any surface finish.

TF-XRD results of HAPEX™ and AWPEX samples at different points throughout SBF incubation are shown in Fig. 5, with data for one- and three-day time points not shown because no change from the initial peak pattern was seen at these points. For HAPEX™, PE peaks decreased in relative intensity after seven days on as-cut surfaces while apatite peaks broadened. No significant change in TF-XRD scan data was seen over the entire 14-day period with polished or grooved samples. For AWPEX, significant change in peak data was seen after seven days for as-cut samples and after 14 days for polished samples, with PE peaks again decreasing in relative intensity, although to a lesser degree than in HAPEX™. In these samples, wollastonite peaks also decreased and apatite peaks broadened.

Results of EDX analysis of HAPEX™ and AWPEX samples at different points throughout SBF incubation are shown in Fig. 6. Little change occurred in polished or grooved HAPEX™ samples over the 14-day period of investigation, but in as-cut HAPEX™, C concentration

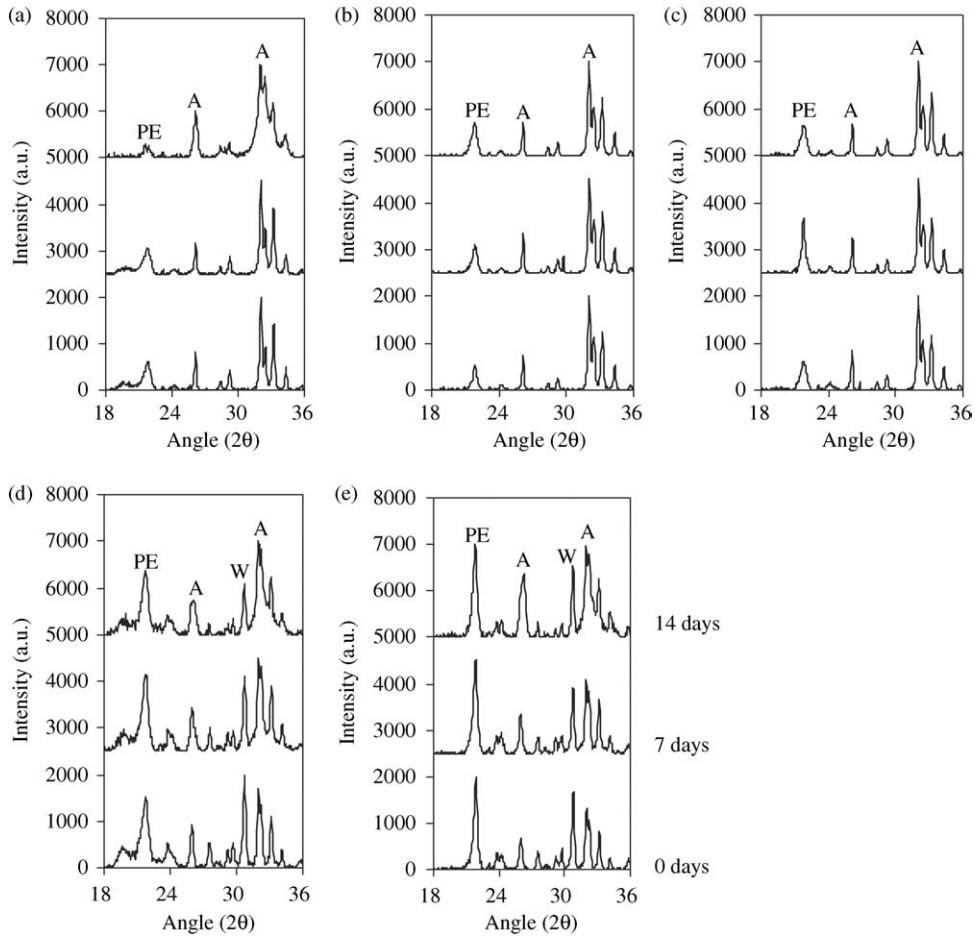

Figure 5 TF-XRD traces of (a) as-cut, (b) polished and (c) grooved HAPEX™ and (d) as-cut and (e) polished AWPEX samples after immersion in SBF. Major peaks identified as apatite (A), wollastonite (W) and polyethylene (PE).

significantly dropped at 14 days while O, Ca and P concentrations increased at the same point. This same change in C, O, Ca and P elements occurred at seven days for as-cut AWPEX and at 14 days for polished AWPEX.

SEM imaging and X-ray mapping of all HAPEX™ samples after one-, three- and seven-day immersion in SBF, and of all AWPEX samples after 1- and 3-day immersion in SBF, were similar to those of the composites prior to SBF exposure (see Figs. 3 and 4), showing no sign of apatite formation and so results for these days are not displayed. However, after seven-day immersion in SBF for as-cut AWPEX (Fig. 7) and after

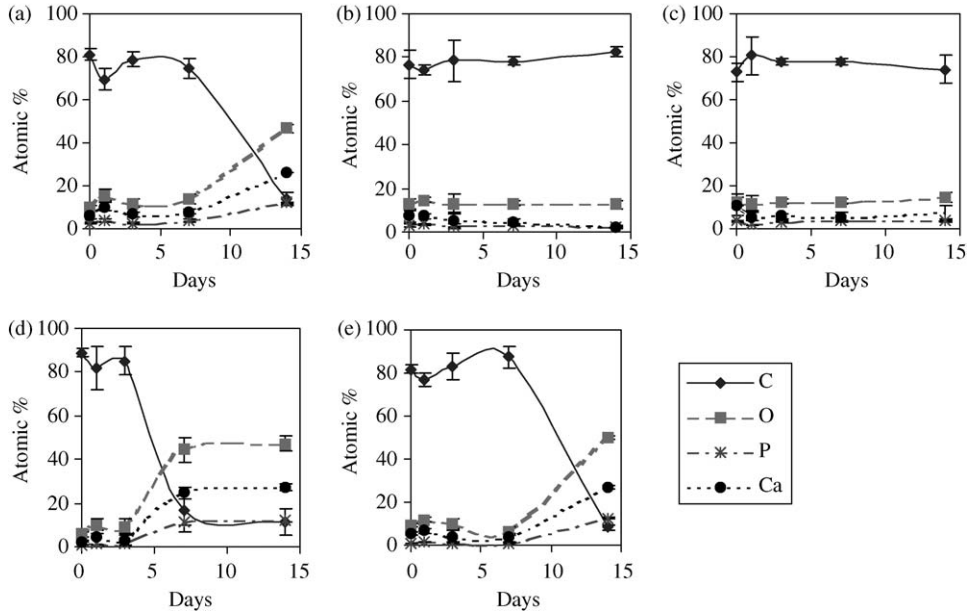

Figure 6 EDX analysis of (a) as-cut, (b) polished and (c) grooved HAPEX™ and (d) as-cut and (e) polished AWPEX samples after immersion in SBF. Data shown as mean ± standard deviation for $N = 5$.

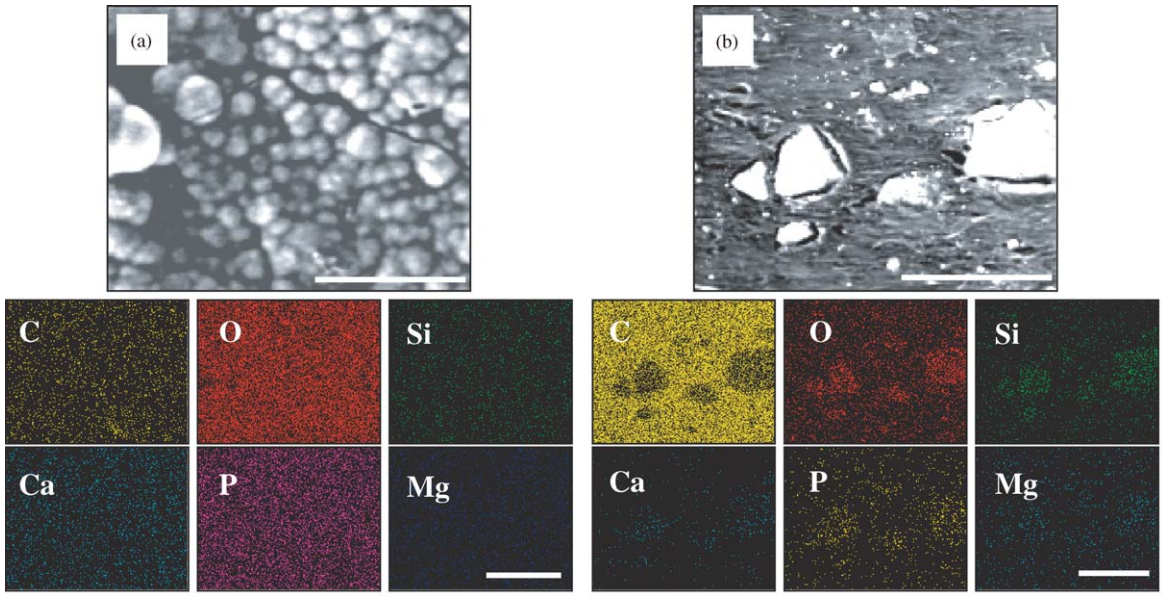

Figure 7 SEM imaging and X-ray mapping of (a) as-cut and (b) polished AWPEX after seven-day immersion in SBF. All scale bars 10 μm.

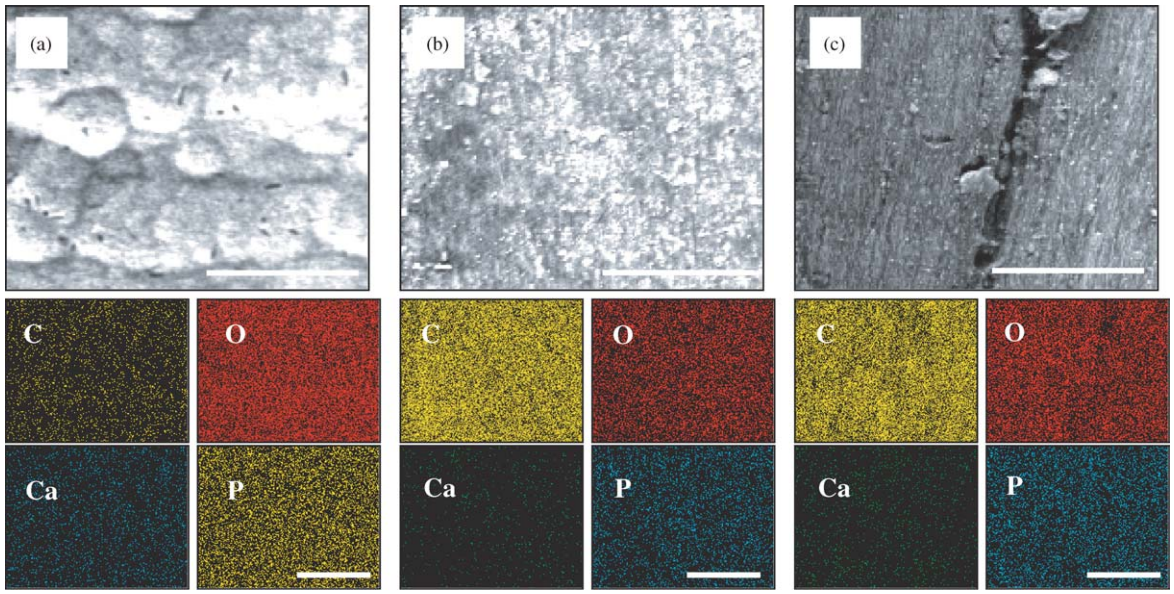

Figure 8 SEM imaging and X-ray mapping of (a) as-cut, (b) polished and (c) grooved HAPEX™ after 14-day immersion in SBF. All scale bars 10 μm.

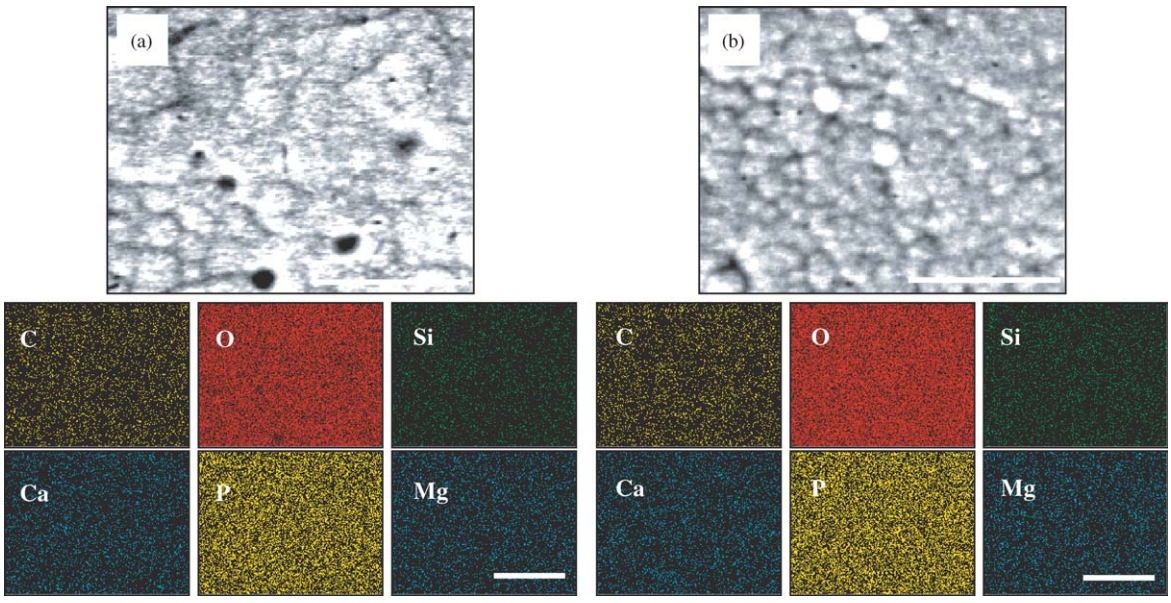

Figure 9 SEM imaging and X-ray mapping of (a) as-cut and (b) polished AWPEX after 14-day immersion in SBF. All scale bars 10 μm.

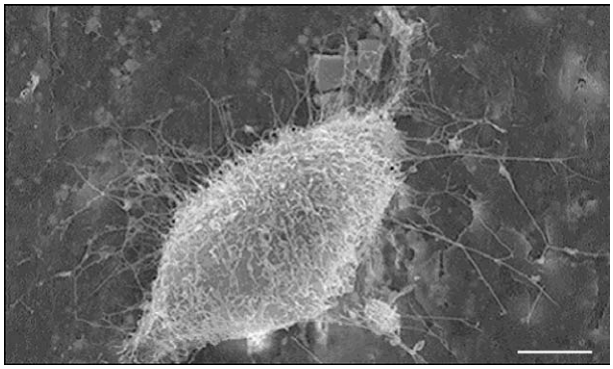

Figure 10 SEM image of cell on polished HAPEX™ surface, seeded at 0.3×10^4 cells/cm^2 and grown for one day. Scale bar 10 μm.

14-day immersion for as-cut HAPEX™ (Fig. 8) and polished AWPEX (Fig. 9), changes were apparent with apatite crystals observed and overall elemental delocalisation with a decrease of C and increase in O, Ca and P content.

3.3. Cell culture and SEM imaging

Osteoblast-like cells were able to attach favorably on both HAPEX™ and AWPEX at all time points examined. A representative secondary electron image of a MG-63 cell seeded on HAPEX™ at low initial cell density (0.3×10^4 cells/cm^2) and grown for a relatively short time period (one day) is given in Fig. 10, to examine the morphology of individual osteoblasts. This cell shows many thin filopodia connecting to the material surface. When seeded at higher density and allowed to grow to near confluence, these filopodia connections extended between cells as well, as shown in Fig. 11. Comparison of secondary electron (Fig. 11(a)) and backscattered electron (Fig. 11(b)) images of such cells illustrates the interaction of the cells with the ceramic HA particles on the composite surface. Preferential attachment of cells to ceramic particles within the PE matrix of each composite was seen, as shown by the secondary electron image in Fig. 12 of a cell, grown at low cell density for short time to allow isolated imaging, on polished AWPEX. Although this image shows possible dehydration or osmotic morphology alteration from the sample preparation technique, the preferential A–W attachment of the cell is clear. Surface topography, as in SBF apatite formation, also affected cell morphology and attachment with cells elongated in the direction of diamond wire saw grooves (Fig. 13).

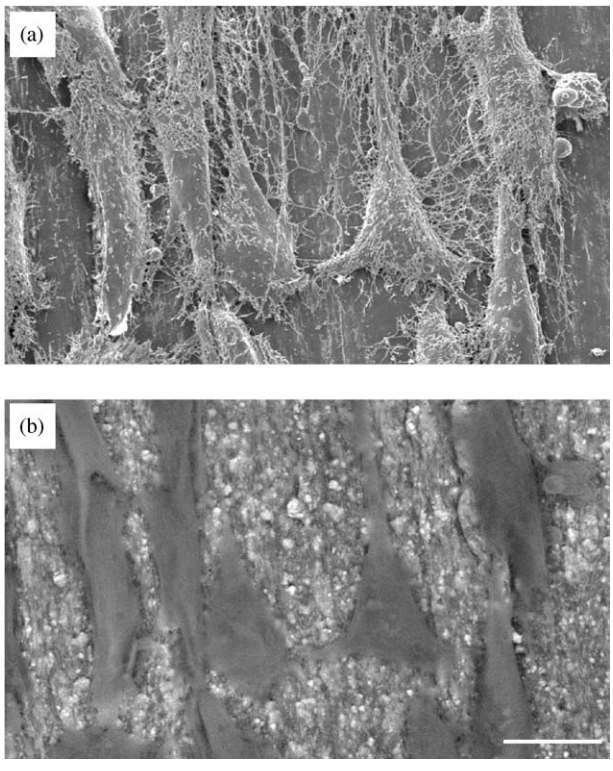

Figure 11 (a) Secondary and (b) back-scattered electron SEM images of cells on HAPEX™ surface, seeded at 2.5×10^4 cells/cm^2 and grown for five days. Scale bar 20 μm.

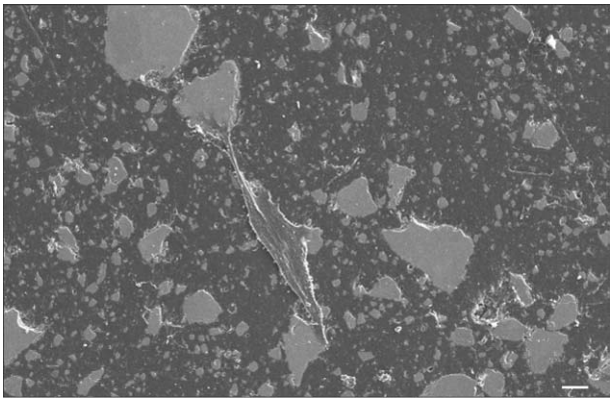

Figure 12 SEM image of cell on polished AWPEX surface, seeded at 0.3×10^4 cells/cm^2 and grown for one day. Scale bar 10 μm.

4. Discussion

The examination of different surface finishes was necessary before beginning *in vitro* SBF or cell studies on the composite materials. The homogenous distribution of HA and glass–ceramic A–W particles within the PE matrix of all composite samples allows valid comparisons between different samples and indicates consistent material properties. A homogeneous dispersion of the filler phase is also critical for high mechanical performance of HAPEX™ and AWPEX as particle agglomeration will reduce overall material strength,

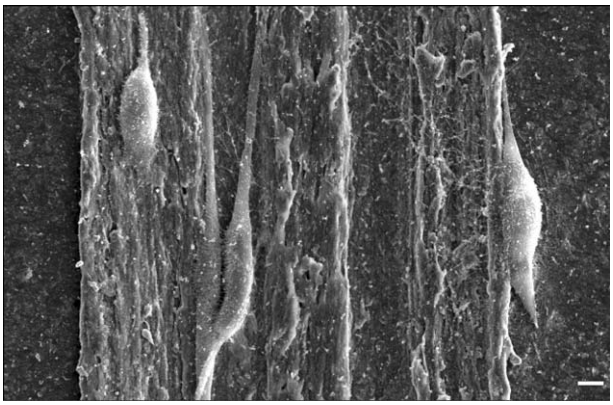

Figure 13 SEM image of cells on grooved HAPEX™ surface, seeded at 0.9×10^4 cells/cm^2 and grown for two days. Scale bar 10 μm.

and so the results seen are positive in this area as well. The significant differences in surface morphology for different surface finishes are also important to consider in terms of effects on apatite formation and cell adhesion.

XRD results of untreated samples showed the presence of expected phases in both composites, with no contaminating phases present and no alteration in crystal structure caused by surface treatments of polishing or groove production. These results verified that any apatite formation subsequently seen is due to the effects of the intended composite components only, and provided a basis for assessment of TF-XRD results later taken for samples incubated with SBF. X-ray mapping results further showed the initial distribution of elements within all materials, important for comparisons and interpretations of X-ray mapping results after incubation of samples in SBF.

Surface roughness measurements provide a useful scale for surface features occurring originally from sample cutting and remaining after polishing steps. The similarities in surface roughness parameters between HAPEX™ and AWPEX samples of the same surface finish indicate that differences seen between such pairs of composites will be due to the inherent composition of the material and not influenced by possible variations in the resistance of the materials to topographic treatment.

The lack of significant change in the pH of the SBF solution during incubation with the composite samples is in accordance with previous studies [15, 16] and indicates that little of the ceramic phase of each composite dissolved into solution over the time period studied. With HA in HAPEX™, which is highly insoluble, little variation is unsurprising. However, the glass–ceramic A–W phase in AWPEX is known to dissolve more readily than HA. It is possible that the volume of SBF used was sufficiently large so that dissolution into the bulk could not be detected. Alternatively, previous SBF study with AWPEX composites, where the SBF solution was analysed by inductively coupled plasma–atomic emission spectroscopy (ICP–AES) after incubation with the material, has indicated that only AWPEX samples containing 50 vol % or more glass–ceramic A–W will release small amounts of magnesium and silicon ions into the surrounding fluid [17]. Therefore, at filler contents below 50 vol %, as used here, minimal change in pH would be expected to occur.

The increase in weight seen for all samples following SBF incubation suggests the deposition of material onto the composite surfaces. The observation that this increase was most pronounced on as-cut samples suggests that as-cut samples were the most responsive in SBF. Initial indications of a greater reactivity for glass–ceramic A–W relative to HA were also seen from the decrease of polished AWPEX sample weight at one day.

The most conclusive evidence for effects of surface composition and topography on bioactivity, however, comes from results of subsequent analytical methods. TF-XRD scanning, SEM imaging, EDX analysis and X-ray mapping all show apatite formation on as-cut AWPEX at seven days, and on as-cut HAPEX™ and polished AWPEX at 14 days. There was no apatite development on polished or grooved HAPEX™ within this time. For the as-cut AWPEX samples, where apatite formation could be seen over two different time points, an increase in apatite layer thickness and crystallinity between seven and 14 days was shown by the continued increase in apatite phase TF-XRD peak height. Furthermore, the broadening of the major apatite peak with increasing SBF immersion time on these and other samples where apatite deposition occurred is characteristic of low crystallinity apatite, which is known to form on the surface of pure glass–ceramic A–W *in vivo* [18] and is due to small crystallites and/or defective structures. The drop in C content observed in EDX analysis of composites with apatite layer growth shows that the PE originally on the surface has been covered, as supported by SEM imaging and X-ray mapping results. The associated rise in O, Ca and P content in EDX data and X-ray mapping reflects the fact that this covering layer must be a calcium phosphate.

In this study, the differences observed between HAPEX™ and AWPEX are most likely due to inherent differences in the bioactivity of HA and glass–ceramic A–W, as the polymer matrix was the same in all composites and previous study has shown PE to be inert as a pure material in SBF [19]. In related work by Juhasz *et al*. [15] and Kokubo *et al*. [17], ICP-AES analysis showed that glass–ceramic A–W alone or in composite form releases appreciable amounts of calcium ions into SBF immediately upon immersion, but HA combined with PE does not, highlighting differences in the solubility of the two ceramic phases examined. Calcium ions released from each composite combine with phosphate ions from the SBF as an apatite layer is formed. In AWPEX, a release of silicon ions from the glass–ceramic A–W phase also occurs [17]. The release of silicon has a role in the formation of apatite in the bone of mammals [20] and has been shown to provide favourable sites for nucleation of the apatite on the surface of glass–ceramic A–W [21] as well as other substrates such as metals and organic polymers [22]. Additionally, Tanahashi *et al*. [23] demonstrated that the presence of silicon can cause apatite to form on the surface of organic polymers, including PE as used for the matrix of HAPEX™ and AWPEX, by a biomimetic process. In this process, silicate ions first combine with calcium ions to form a calcium silicate on the substrate surface. Phosphate ions from the SBF then displace the silicate to form an amorphous calcium phosphate and eventually transform into crystalline apatite.

However, the differences in bioactivity between composites may also be partially due to effects of the filler particle morphology. As seen previously, HA particles have smooth surfaces at a sub-microscopic level with nodular protrusions of $\sim 0.5\,\mu m$, while glass–ceramic A–W particles possess angular surfaces on a macroscopic scale [15]. HA particles are nodular because they are created from agglomerates of smaller particles. Furthermore, the broader distribution of particle size for the glass–ceramic A–W used to make AWPEX in comparison to that of the HA used to make HAPEX™ gives a greater packing efficiency for glass–ceramic A–W, with smaller particles available to fill gaps between particles of larger size. Greater ion dissolution therefore may occur, accelerating apatite growth. These differ-

ences may also affect the attachment and development of cells on the composite surfaces.

Osteoblast-like cell culture results provide a complement to SBF findings. Previous studies on HAPEX™ alone have shown that material surface topography has a large influence on cell proliferation and attachment [24], with osteoblasts attaching in greater numbers to a polished then roughened surface than a surface left as originally machined [25]. The observed preferential attachment of cells to the ceramic components of HAPEX™ and AWPEX is in accordance with previous findings on similar composites [26, 27] and further indicates the bioactivity of HA and glass–ceramic A–W. This cell behaviour was especially predominant on AWPEX samples, possibly linked to the higher bioactivity seen with these composites in incubation with SBF. Both materials favour cell attachment but more quantitative cell culture investigations are necessary to determine the effect of each material on osteoblast proliferation and matrix production. Furthermore, the observed contact guidance of cells seeded on patterned surfaces, particularly the alignment of cells with parallel groove formations, has been reported for other materials as well [28], and could be of use for implant design. These results highlight areas for continued investigation.

5. Conclusions

The findings of this study show that, at ceramic filler content of 40 vol %, AWPEX has a higher level of bioactivity than HAPEX™. Surface topography also influences apatite formation, with increased roughness allowing more nucleation sites and hence more rapid apatite development than samples that have been highly polished. Both materials are favourable for osteoblast-like cell growth, with preferential attachment to ceramic particles within the composite matrices and contact guidance effects from surface topography.

Acknowledgments

The British Marshall Scholarship, National Science Foundation, ApaTech Ltd., and NCAA Postgraduate Scholarship programs are thanked for their financial support. Thanks also to Dr J. Skepper and Dr T. Burgess for assistance with cell imaging, the Interdisciplinary Research Centre in Biomedical Materials, London, UK for provision of HAPEX™ and Professor T. Kokubo for arranging the provision of AWPEX composites.

References

1. W. BONFIELD, *J. Biomed. Eng.* **10** (1988) 522.
2. M. WANG, T. KOKUBO and W. BONFIELD, *Bioceramics* **9** (1996) 387.
3. R. N. DOWNES, S. VARDY, K. E. TANNER and W. BONFIELD, *ibid.* **4** (1991) 239.
4. H. L. DORNHOFFER, *Laryngoscope* **108** (1998) 531.
5. T. KOKUBO, *Biomaterials* **12** (1991) 155.
6. L. L. HENCH, *Bioceramics* **7** (1994) 3.
7. M. E. HOLTROP, in ''Bone: Volume I. The Osteocyte'', edited by B. K. Hall (The Telford Press, New Jersey, 1990) p. 1.
8. D. A. PULEO and A. NANCI, *Biomaterials* **20** (1999) 2311.
9. T. ALBREKTSSON, in ''Implant Bone Interface'', edited by J. Older (Springer-Verlag, London, 1990) p. 7.
10. J. E. DAVIES, *Anatom. Record* **245** (1996) 426.
11. T. KOKUBO, H. KUSHITANI, S. SAKKA, T. KITSUGI and T. YAMAMURO, *J. Biomed. Mater. Res.* **24** (1990) 721.
12. K. O. MUHAMMED, C. OZENER and E. AKOGLU, *Periton. Dialysis Int.* **21** (2001) 154.
13. V. M. HITCHINS and K. MERRITT, *J. Biomed. Mater. Res.* **46** (1999) 434.
14. M. J. DALBY, L. DI SILVIO, N. GURAV, B. ANNAZ, M. V. KAYSER and W. BONFIELD, *Tiss. Eng.* **8** (2002) 453.
15. J. A. JUHASZ, S. M. BEST, M. KAWASHITA, N. MIYATA, T. KOKUBO, T. NAKAMURA and W. BONFIELD, *Bioceramics* **14** (2001) 437.
16. J. HUANG, L. DI SILVIO, M. WANG and W. BONFIELD, *J. Mater. Sci.: Mater. Med.* **8**, (1997) 775.
17. T. KOKUBO, H. KUSHITANI, C. OHTSUKI, S. SAKKA and T. YAMAMURO, *ibid.* **3** (1992) 79.
18. T. KITSUGI, T. NAKAMURA, T. YAMAMURO, T. KOKUBO, T. SHIBUYA and T. TAKAGI, *J. Biomed. Mater. Res.* **21** (1987) 1255.
19. J. A. JUHASZ, S. M. BEST, M. KAWASHITA, N. MIYATA, T. KOKUBO, T. NAKAMURA and W. BONFIELD, *Biomaterials* **25** (2004) 949.
20. E. M. CARLISLE, *Science* **167** (1970) 279.
21. T. KOKUBO, *J. Non-Cryst. Solids* **120** (1990) 138.
22. H. TAKADAMA, H.-M. KIM, F. MIYAJI, T. KOKUBO and T. NAKAMURA, *J. Ceram. Soc. Jpn.* **108** (2000) 118.
23. M. TANAHASHI, T. YAO, T. KOKUBO, M. MINODA, T. MIYAMOTO, T. NAKAMURA and T. YAMAMURO, *J. Am. Ceram. Soc.* **77** (1994) 2805.
24. M. J. DALBY, L. DI SILVIO, G. DAVIES and W. BONFIELD, *J. Mater. Sci.: Mater. Med.* **12** (2000) 805.
25. M. J. DALBY, M. V. KAYSER, W. BONFIELD and L. DI SILVIO, *Biomaterials* **23** (2002) 681.
26. W. BONFIELD, M. WANG and K. E. TANNER, *Acta Mater.* **46** (1998) 2509.
27. S. C. RIZZI, D. J. HEATH, A. G. COOMBES, N. BOCK, M. TEXTOR and S. DOWNES, *J. Biomed. Mater. Res.* **55** (2001) 475.
28. Y. A. ROVENSKY, I. L. SLAVNAJA and J. M. VASILEV, *Exp. Cell Res.* **65** (1971) 193.

Received 9 September 2003
and accepted 26 February 2004